NASA TECHNICAL NOTE

NASA TN D-5526




# CONVECTIVE HEAT-TRANSFER RATES ON LARGE-ANGLE CONICAL BODIES AT HYPERSONIC SPEEDS

*by David A. Stewart and Joseph G. Marvin*

*Ames Research Center*
*Moffett Field, Calif.*

NATIONAL AERONAUTICS AND SPACE ADMINISTRATION • WASHINGTON, D. C. • NOVEMBER 1969

| 1. Report No. NASA TN D-5526 | 2. Government Accession No. | 3. Recipient's Catalog No. |
|---|---|---|
| 4. Title and Subtitle<br>CONVECTIVE HEAT-TRANSFER RATES ON LARGE-ANGLE CONICAL BODIES AT HYPERSONIC SPEEDS | | 5. Report Date<br>November 1969<br>6. Performing Organization Code |
| 7. Author(s)<br>David A. Stewart and Joseph G. Marvin | | 8. Performing Organization Report No.<br>A-3411 |
| 9. Performing Organization Name and Address<br>NASA Ames Research Center<br>Moffett Field, Calif. 94035 | | 10. Work Unit No.<br>124-07-02-32-00-21<br>11. Contract or Grant No.<br>13. Type of Report and Period Covered<br>Technical Note |
| 12. Sponsoring Agency Name and Address<br>National Aeronautics and Space Administration<br>Washington, D. C. 20546 | | 14. Sponsoring Agency Code |

15. Supplementary Notes

16. Abstract

Heat-transfer rates were measured on large-angle conical bodies with large half-angles ($\delta$) between $50^{\circ}$ and $90^{\circ}$, at angles of attack from $0^{\circ}$ to $30^{\circ}$. The results at $0^{\circ}$ angle of attack were predicted with Lees' similarity theory, using calculated flow properties at the boundary-layer edge. The calculated flow properties were obtained from Newtonian theory for the $50^{\circ}$ cone and from a one- or two-strip solution using the method of integral relations for the other cones. At $0^{\circ}$ angle of attack, an increase in cone angle resulted in a decrease in the heating rate over much of the body. However, high heating rates occurred at the shoulder of both the $\delta = 80^{\circ}$ and $\delta = 90^{\circ}$ shapes because of local pressure gradients. On the windward side of the cones, the heating rate increased with angle of attack.

| 17. Key Words Suggested by Author(s) | 18. Distribution Statement |
|---|---|
| Convective heat transfer<br>Blunt bodies<br>Cones<br>Large angle | Unclassified - Unlimited |

| 19. Security Classif. (of this report) | 20. Security Classif. (of this page) | 21. No. of Pages | 22. Price* |
|---|---|---|---|
| Unclassified | Unclassified | 13 | $3.00 |

*For sale by the Clearinghouse for Federal Scientific and Technical Information
Springfield, Virginia 22151

## SYMBOLS

| | |
|---|---|
| $c_p$ | specific heat of model material |
| H | total enthalpy |
| M | Mach number |
| p | pressure |
| $\dot{q}$ | heating rate |
| R | radius |
| $Re_D$ | Reynolds number (free-stream Reynolds number based on diameter) |
| $\bar{r}$ | radius of cross section of body of revolution |
| s | surface distance from center of nose |
| $s_c$ | surface distance from center of nose to center of shoulder |
| T | absolute temperature |
| t | time |
| u | velocity |
| $\alpha$ | angle of attack |
| $\delta$ | cone half-angle |
| $\rho$ | density |
| $\tau$ | model skin thickness |

### Subscripts

| | |
|---|---|
| b | body |
| c | shoulder |
| e | outer edge of the boundary layer |
| hemi | hemisphere stagnation point |
| n | nose |
| st | model stagnation point |

| | |
|---|---|
| t | isentropic stagnation condition |
| w | model wall condition |
| $\infty$ | free stream |
| 1 | nose sphere-cone junction |
| 2 | cone-shoulder radius junction |

# CONVECTIVE HEAT-TRANSFER RATES ON LARGE-ANGLE CONICAL BODIES AT HYPERSONIC SPEEDS

By David A. Stewart and Joseph G. Marvin

Ames Research Center

## SUMMARY

Heat-transfer rates were measured on large-angle conical bodies with large half-angles ($\delta$) between 50° and 90°, at angles of attack from 0° to 30°. The results of 0° angle of attack were predicted with Lees' similarity theory, using calculated flow properties at the boundary-layer edge. The calculated flow properties were obtained from Newtonian theory for the 50° cone and from a one- or two-strip solution using the method of integral relations for the other cones. At 0° angle of attack, an increase in cone angle resulted in a decrease in the heating rate over much of the body. However, high heating rates occurred at the shoulder of both the $\delta$ = 80° and $\delta$ = 90° shapes because of local pressure gradients. On the windward side of the cones, the heating rate increased with angle of attack.

## INTRODUCTION

Large angle cones are being considered for planetary probe configurations. Methods for predicting the surface pressures, shock-wave shapes, and aerodynamics of this class of bodies are necessarily complex because the flow is no longer conical. Much has been done experimentally to provide data on the character of the inviscid flow over these bodies and the data can be used to substantiate prediction techniques (see, e.g., refs. 1-6). The probe designer must also be able to predict the convective heating to these bodies. However, experimental heating data for substantiating any prediction methods for this class of bodies are lacking. To partially fill this need an investigation was initiated in the Ames 42-inch shock tunnel to provide convective heat-transfer data. The investigation was performed at a Mach number of 15 in air with cone semivertex angles ranging from 50° to 90°. The results of this investigation are presented herein.

## APPARATUS AND TEST CONDITIONS

### Facility

The tests were conducted in the Ames 42-inch shock tunnel (refs. 7 to 10). This facility uses combustion-heated driver gas to produce a reflected shock, tailored-interface reservoir of test gas at the end of a 40-foot-long, 6.2-inch-diameter shock tube. Initial values of reservoir pressure and

enthalpy were 286 atmospheres and 4000 Btu/lbm. The reservoir gas (air for the present tests) was expanded through a 20° conical nozzle to generate a flow in the test region having a Mach number of 15 and a velocity of 13,600 feet per second. The corresponding Reynolds number, based on model diameter, was 6700. The flow duration for each test was 20 milliseconds.

## Models

The models (fig. 1) were cone-cylinders with a spherical nose cap, and a shoulder radius joining the conical section to a short cylindrical afterbody. The ratios of nose radius to body radius, and shoulder radius to body radius, were 0.10 and 0.05, respectively. The forebodies included cones with half-angles of 50°, 60°, 70°, and 80°, and a flat-faced cylinder. The models were made of copper and had nominal wall thicknesses of 0.017 inch. Thermocouples were located along a single ray from the stagnation point to the center of the shoulder radius. Thermocouples were also located on the cylindrical afterbody of the 80° cone and the flat-faced cylinder. Each thermocouple was made by drilling two small holes 0.02 inch apart in the model wall and soldering a pair of chromel-constantan No. 40 gage wire in these holes.

A 1-inch-diameter hemisphere, which provided a monitor measurement of stagnation-point heat-transfer rate, was also located in the test region. It was located 12 inches off the centerline of the test section and did not interfere with the flow over the model. This hemisphere was also made of copper but had a wall thickness of 0.007 inch. It was instrumented with a chromel-constantan thermocouple in the same manner as the models.

## Data Reduction

The heat-transfer data were obtained by measuring the increase of model wall temperature as indicated by the thermocouples during a test of approximately 20 msec. Thermocouple outputs were amplified and recorded on a high-speed oscillograph. The temperature-time data were curve-fitted with a seventh-order polynomial. Heat-transfer rates at a given time were determined from the equation,

$$\dot{q} = \rho c_p \tau (dT/dt) \qquad (1)$$

The estimated maximum error in $\dot{q}$ was ±10 percent. Further details regarding the data reduction and testing techniques are available in reference 10.

Because the heating rates determined from equation (1) changed over the test time as a result of changes in the reservoir conditions, the measured heating rate to the monitor hemisphere was used to normalize the test data. This normalization resulted in a constant heating rate ratio over the usable test time. Furthermore, it minimized small differences in heating-rate level between runs that occurred because the test conditions could not be precisely repeated.

## RESULTS AND DISCUSSION

Before the heat-transfer data are examined in detail, the flow field over large-angle cones will be discussed briefly and some equations used to predict the heating rates will be presented.

Increasing the cone angle beyond the detachment angle for a pointed cone (e.g., $\delta = 58°$ for ideal air) causes significant changes in the inviscid flow. For example, the bow wave over the conical portion of the cone changes from conical to spherical and the flow along the cone surface changes from supersonic to subsonic (ref. 5). The inviscid subsonic shock-layer flow can no longer be predicted by Newtonian theory as suggested by Lees in his study on heating to blunt cones (see ref. 11). However, as shown in references 4 and 5, the inviscid flow over large-angle cones can be predicted by the method of integral relations. For this method, the shock layer is divided into strips concentric with the body, and the flow properties across the strips are represented by polynomials. The inviscid flow properties are then obtained by numerically solving the governing conservation equations. The degree of the polynomial depends on the number of strips. More details of this method may be found in reference 12. For the present investigation, one- and two-strip solutions were obtained for the cones with half-angles greater than 60°. For the 60° cone, only a one-strip solution was possible because of numerical difficulties.

Once the inviscid flow over the cones has been determined, one may apply the theory proposed by Lees to predict the cone heating distribution. The following equation can be formulated:

$$\dot{q}/\dot{q}_{hemi} = (\dot{q}/\dot{q}_{st})_{Lees}(\dot{q}_{st}/\dot{q}_{hemi}) \tag{2}$$

where

$$\left(\frac{\dot{q}}{\dot{q}_{st}}\right)_{Lees} = \frac{(p/p_{st})(u_e/u_\infty)\bar{r}}{2\left[\int_o^s (p/p_{st})(u_e/u_\infty)\bar{r}^2\, ds\right]^{1/2}\left[(1/u_\infty)(du_e/ds)_{st}\right]^{1/2}} \tag{2a}$$

and

$$\frac{\dot{q}_{st}}{\dot{q}_{hemi}} = \sqrt{\frac{(du_e/ds)_{st}}{(du_e/ds)_{hemi}}} \tag{2b}$$

The heating rate has been made dimensionless by the stagnation-point heating rate of a hemisphere to be consistent with the previously mentioned data normalization. The heating rate to the hemisphere can be obtained from the following equation taken from reference 13.

$$\dot{q}_{st} = 86.9\sqrt{\frac{p_{st}}{R_n}}\left(\frac{u_\infty}{10{,}000.0}\right)^{1.99}\left(1 - \frac{H_w}{H_t}\right) \tag{3}$$

where $R_n$ is the radius of the hemisphere. In the derivation of equation (3), a Newtonian velocity gradient was assumed at the stagnation point, that is,

$$\left(\frac{du_e}{ds}\right)_{st} = \frac{1}{R_n}\sqrt{\frac{2p_{st}}{\rho_{st}}} \tag{4}$$

## Stagnation-Point Heating Rate

The measured stagnation-point heating-rate ratio is plotted in figure 2 as a function of cone angle. There is a significant decrease in cone stagnation-point heating with increasing cone angle. Also shown are the ratios predicted by equation (2b). The prediction represented by the broken line was based on Newtonian velocity gradients for the hemisphere and the cones out to $\delta = 58°$ (the pointed cone detachment angle for inviscid flow theory with $\gamma = 1.4$). Therefore, the predicted value is simply the square root of the ratio of the hemisphere and cone-nose radii (see, eq. (4)). The agreement with the measured ratio at $\delta = 50°$ is very good. For cone angles of 60° and larger, the method of integral relations was used to obtain the cone stagnation-point velocity gradients in equation (2b) from one-strip (solid line) and two-strip (dashed line) solutions. The data agree well with the ratio formed by the more accurate, two-strip solution. The results in figure 2 demonstrate that the changes in stagnation-point heating rate with cone angle are due mainly to changes in stagnation-point velocity gradient. Therefore, equation (3) in combination with an appropriate velocity gradient ratio can be used to predict the stagnation-point heating.

## Heating-Rate Distribution

Zero angle of attack.- The heating-rate distributions at 0° angle of attack are given in figure 3. Data from two test runs are presented for each cone angle. As the cone angle increases, the heating rates decrease markedly for $s/s_c < 0.5$. For $s/s_c > 0.5$, there is little change except in the vicinity of the shoulder for both the 80° cone and the flat-faced cylinder. In this region, the heating rates exceed their respective stagnation-point values. To obtain the lines on figure 3, equation (2) was used with the appropriate inviscid flow-field quantities from Newtonian theory ($\delta = 50°$) and the method of integral relations ($\delta \geq 60°$). The 50° cone data (fig. 3(a))

compare well with the heating-rate distribution predicted by equation (2) with a Newtonian approximation for the inviscid flow-field properties. The 60° cone data (fig. 3(b)) compare well with the heating-rate distribution predicted by a one-strip solution for the inviscid flow properties in equation (2). The data for $\delta > 60°$ (figs. 3(c) to 3(e)) compare better with the two-strip solution because the one-strip solution does not adequately predict the inviscid flow in the stagnation region. The differences between theory and experiment on the shoulder regions of the 80° cone are attributed to a combination of two factors: (1) the theory neglects pressure gradient effects (e.g., see ref. 6), and (2) the experimental measurements on the small shoulder radii are uncertain. It was expected that these factors also would influence the comparison for $\delta = 90°$, but this is not evidenced in the data.

Angle of attack to 30°.- Windward heat-transfer data on the 50°, 60°, and 70° cones, for angles of attack between 0° and 30°, are shown in figure 4. Note that $s/s_c = 0$ is the location of the geometric center of the spherical nose cap. Lines have been faired through the data to aid in the interpretation. On the 50° and 60° cones, the heat transfer at $s/s_c = 0$ decreases, and the heating rates along the conical sections increase with increasing angle of attack (figs. 4(a) and 4(b)). On the 70° cone, differences in heating rates at $s/s_c = 0$ are small with increasing angle of attack except at $\alpha = 30°$. At this large angle the heating rate decreases markedly, as might be expected, since the spherical cap is swept with respect to the incident stream. The trend near the shoulder of the 70° cone is similar to that of the 50° and 60° cones. However, the heating along the middle of the 70° cone conical section decreases with increasing angle of attack. No attempt was made to predict the heating rate at angle of attack because of the complexity of the flow field.

## CONCLUSIONS

A study of convective heating rates on blunted cones with cone half-angles between 50° and 90° in air at Mach 15 resulted in the following observations:

1. At 0° angle of attack, an increase in cone angle resulted in a decrease in the heating rate level over most of the test model, especially at the stagnation point. Decreases in stagnation-point heating were adequately estimated by accounting for decreases in stagnation-point velocity gradient.

2. At the shoulder of the 80° cone and the flat-faced cylinder, the heating rates were higher than at the stagnation point, probably because of the influence of large local pressure gradients.

3. In general, Lees' similarity theory used in conjunction with estimated pressure distributions adequately predicted heating rates over the surface of the models at 0° angle of attack.

4. With increasing angle of attack, the heating rates to the 50°, 60°, and 70° cones increased on the windward surface. An exception to this behavior was the 70° cone on which the heating rates decreased near the middle of the conical section with increasing angle of attack.

Ames Research Center
National Aeronautics and Space Administration
Moffett Field, Calif., 94035, Aug. 12, 1969

## REFERENCES

1. Johnson, Robert H.: The Cone-Sphere in Hypersonic Helium Above Mach 20. Aerospace Engineering, vol. 2, no. 4, Feb. 1959, pp. 30-34.

2. Saida, Nobumi: Supersonic Flow Around Blunt Cones at Small Angles of Attack. Japan Society for Aeronautical and Space Sciences, Transactions, vol. 8, no. 13, 1965, pp. 45-53.

3. Walker, Billy; and Weaver, Robert W.: Static Aerodynamic Characteristics of Blunted Cones in the Mach-Number Range From 2.2 to 9.5. NASA CR 94553, 1967.

4. Campbell, James F.; and Tudor, Dorothy H.: Pressure Distributions on 140°, 160°, and 180° Cones at Mach Numbers From 2.30 to 4.63 and Angles of Attack From 0° to 20°. NASA TN D-5204, 1969.

5. Stewart, David A.; and Inouye, Mamoru: Shock Shapes and Pressure Distributions for Large-Angle Pointed Cones in Helium at Mach Numbers of 8 and 20. NASA TN D-5343, 1969.

6. Marvin, Joseph G.; and Sinclair, Richard A.: Convective Heating in Regions of Large Favorable Pressure Gradient. AIAA J., vol. 5, no. 11, Nov. 1967, pp. 1940-1948.

7. Loubsky, William J.; Hiers, Robert S.; and Stewart, David A.: Performance of a Combustion Driven Shock Tunnel With Application to the Tailored-Interface Operating Conditions. Presented at the 3rd Conference on Performance of High Temperature Systems, Dec. 7-9, 1964, Pasadena, Calif.

8. Stewart, David A.; and Dannenberg, Robert E.: A Note on Wire Ignition in Combustion-Heated Drivers for Shock Tunnel Application. NASA TN D-3063, 1965.

9. Dannenberg, Robert E.; and Stewart, David A.: Techniques for Improving the Opening of the Main Diaphragm in a Large Combustion Driver. NASA TN D-2735, 1965.

10. Hiers, Robert S., Jr.; and Reller, John O., Jr.: Analysis of Nonequilibrium Air Streams in the Ames 1-Foot Shock Tunnel. NASA TN D-4985, 1969.

11. Lees, Lester: Laminar Heat Transfer Over Blunt-Nosed Bodies at Hypersonic Flight Speed. Ramo-Wooldridge Corp. N-42601, Nov. 1955.

12. Inouye, Mamoru; Marvin, Joseph G.; and Sinclair, A. Richard: Comparison of Experimental and Theoretical Shock Shapes and Pressure Distributions on Flat-Faced Cylinders at Mach 10.5. NASA TN D-4397, 1968.

13. Marvin, Joseph G.; and Akin, Clifford M.: Pressure and Convective Heat-Transfer Measurements in a Shock Tunnel Using Several Test Gases. NASA TN D-3017, 1965.

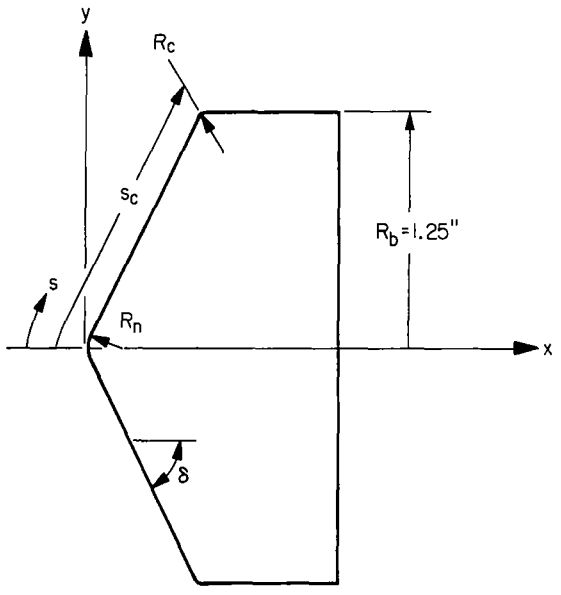


Figure 1.- Typical blunted cone configuration.

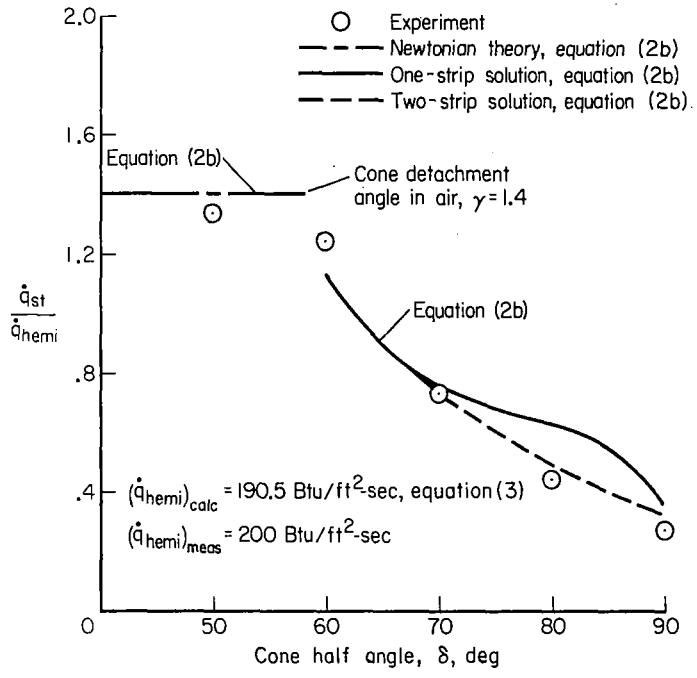


Figure 2.- Variation of stagnation-point heating rate with cone angle.

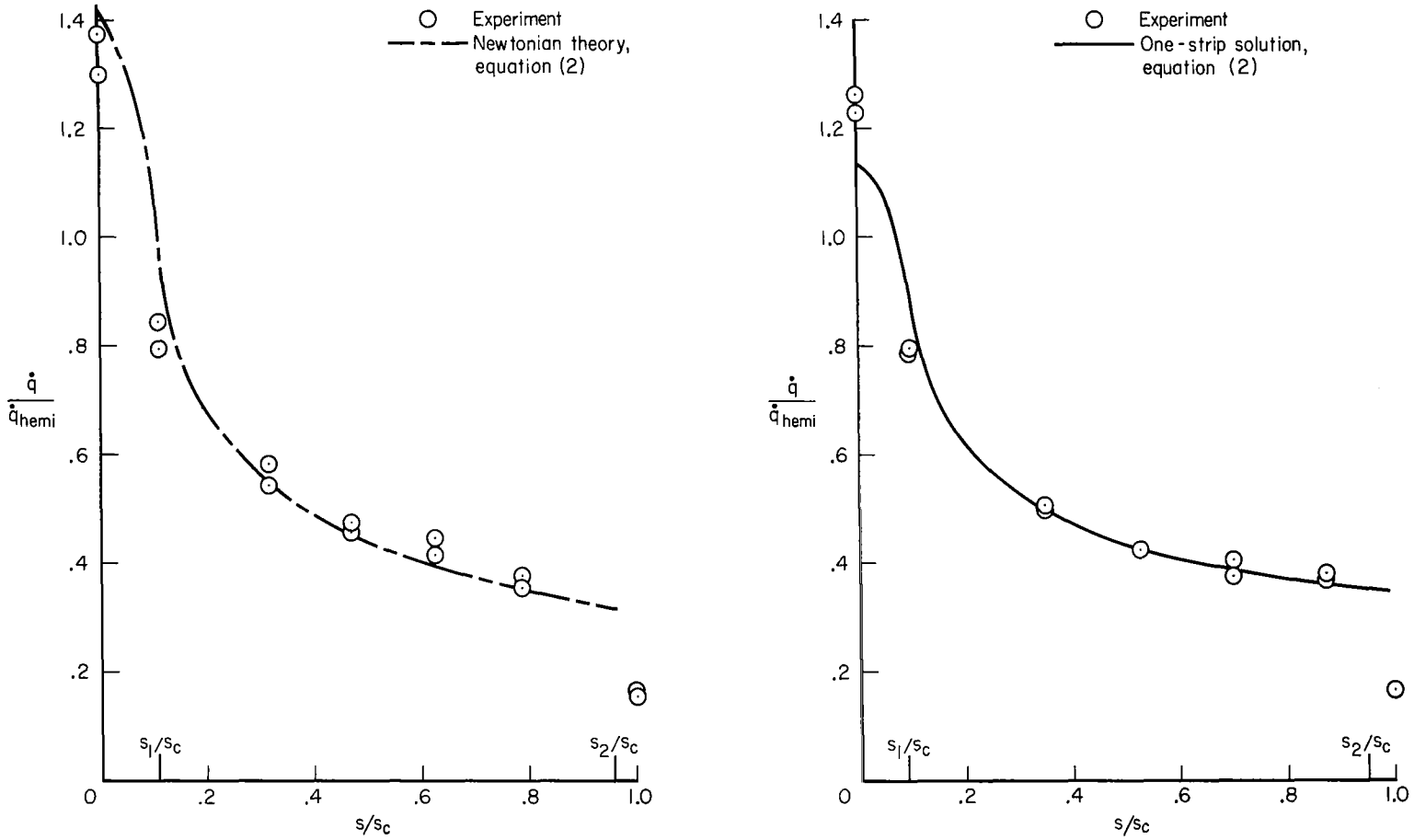


(a) $\delta = 50^\circ$ (b) $\delta = 60^\circ$

Figure 3.- Convective heat-transfer distribution over large-angle conical bodies at $\alpha = 0^\circ$.

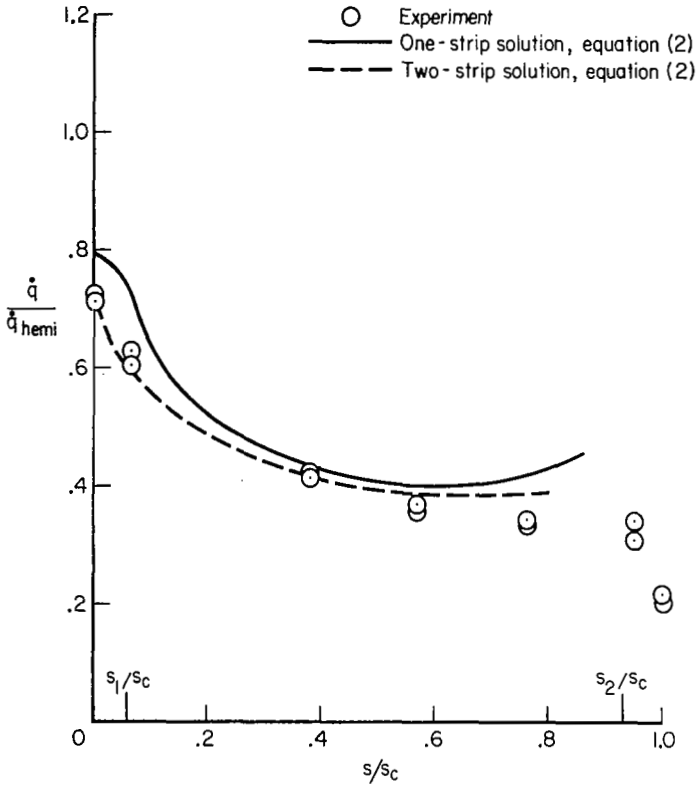


(c) $\delta = 70^{\circ}$

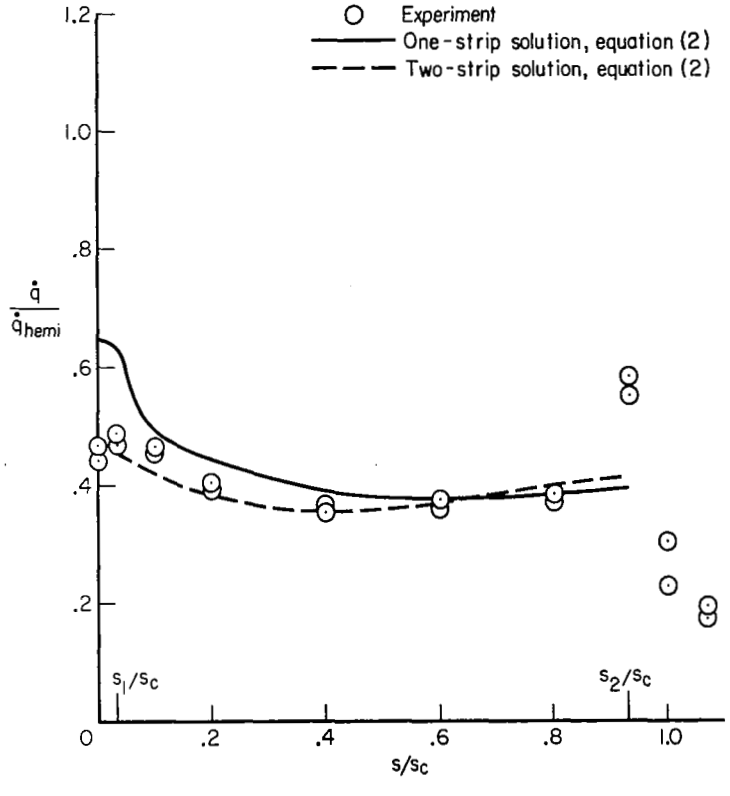


(d) $\delta = 80^{\circ}$

Figure 3.- Continued.

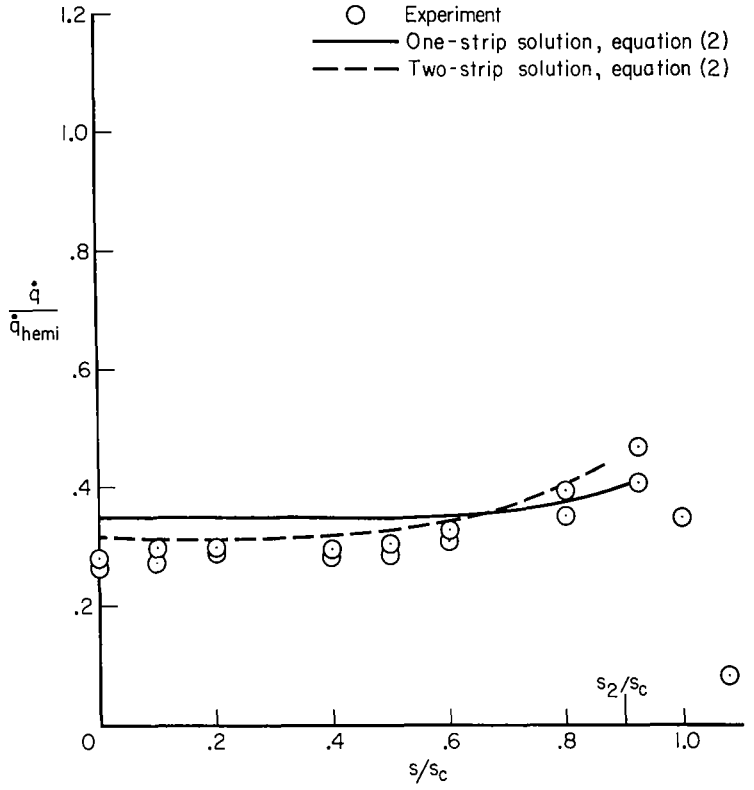


(e) $\delta = 90^\circ$

Figure 3.- Concluded.

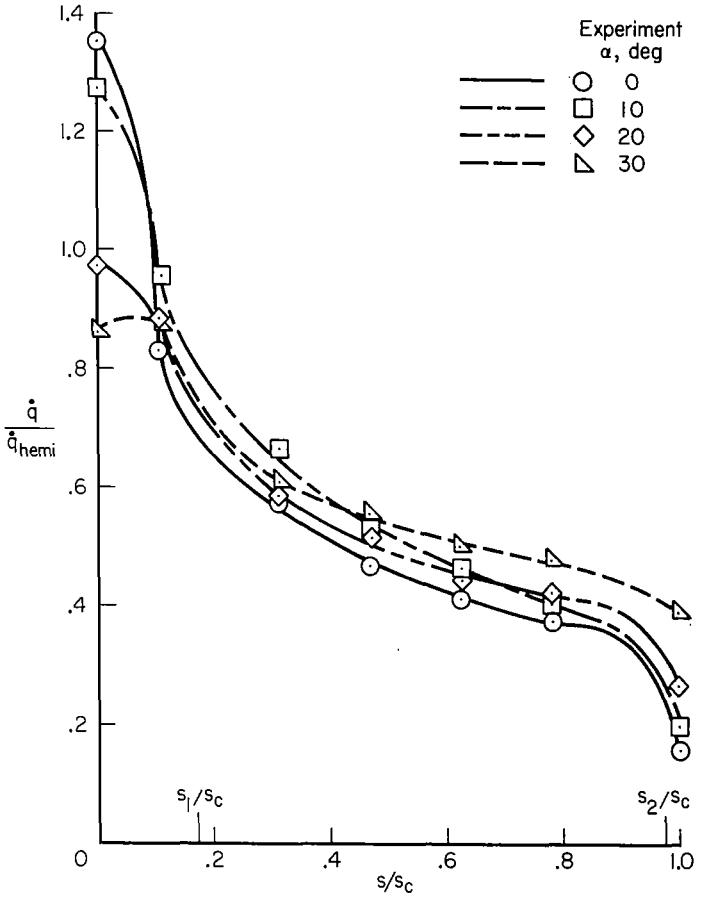


(a) $\delta = 50^\circ$

Figure 4.- Convective heating rates on windward side of conical bodies at angles of attack from $0^\circ$ to $30^\circ$.

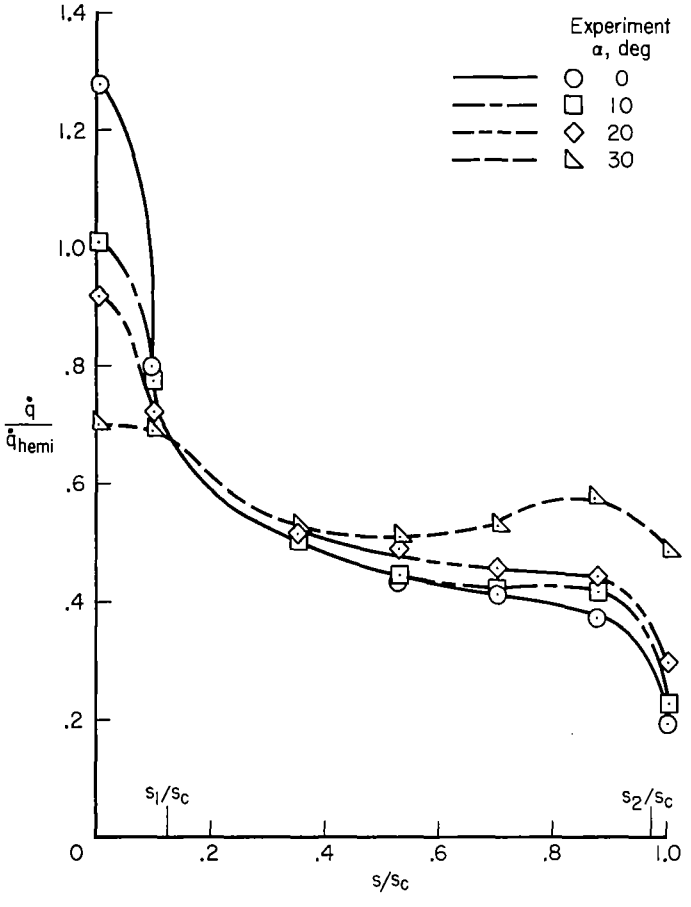


(b) $\delta = 60^\circ$

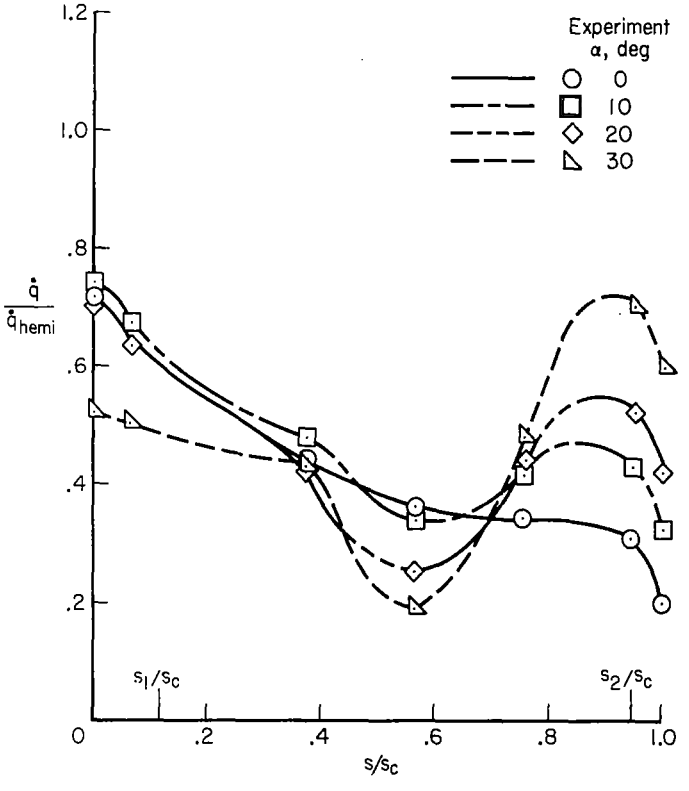


(c) $\delta = 70^\circ$

Figure 4.- Concluded.

NATIONAL AERONAUTICS AND SPACE ADMINISTRATION
WASHINGTON, D. C. 20546
OFFICIAL BUSINESS

FIRST CLASS MAIL

POSTAGE AND FEES PAID
NATIONAL AERONAUTICS AN
SPACE ADMINISTRATION



*"The aeronautical and space activities of the United States shall be conducted so as to contribute . . . to the expansion of human knowledge of phenomena in the atmosphere and space. The Administration shall provide for the widest practicable and appropriate dissemination of information concerning its activities and the results thereof."*

—NATIONAL AERONAUTICS AND SPACE ACT OF 1958

# NASA SCIENTIFIC AND TECHNICAL PUBLICATIONS

TECHNICAL REPORTS: Scientific and technical information considered important, complete, and a lasting contribution to existing knowledge.

TECHNICAL NOTES: Information less broad in scope but nevertheless of importance as a contribution to existing knowledge.

TECHNICAL MEMORANDUMS: Information receiving limited distribution because of preliminary data, security classification, or other reasons.

CONTRACTOR REPORTS: Scientific and technical information generated under a NASA contract or grant and considered an important contribution to existing knowledge.

TECHNICAL TRANSLATIONS: Information published in a foreign language considered to merit NASA distribution in English.

SPECIAL PUBLICATIONS: Information derived from or of value to NASA activities. Publications include conference proceedings, monographs, data compilations, handbooks, sourcebooks, and special bibliographies.

TECHNOLOGY UTILIZATION PUBLICATIONS: Information on technology used by NASA that may be of particular interest in commercial and other non-aerospace applications. Publications include Tech Briefs, Technology Utilization Reports and Notes, and Technology Surveys.

*Details on the availability of these publications may be obtained from:*

**SCIENTIFIC AND TECHNICAL INFORMATION DIVISION**

**NATIONAL AERONAUTICS AND SPACE ADMINISTRATION**

**Washington, D.C. 20546**